Supplementary Figure Legend

Figure S1. AMPK-pathway related genes are enriched in parietal cells, Related to Figure 1

A. Pure populations of parietal and non-parietal cells were sorted by flow cytometry of gastric epithelial cells from *Atp4b-cre;Rosa;mT/mG* mice.
B. Expression Profiles (Affymetrix GeneChip) of flow-sorted parietal cells vs non-parietal gastric cells were analyzed by gene set enrichment analysis (GSEA). GO Genesets with highest Normalized Enrichment Score (NES) in parietal cell VS non-parietal cells were shown, Figure 1, Panel (A): GO_ Mitochondrial Complex1 Biogenesis
C. GSEA for GO_ Oxidative Phosphorylation as for Panel (A)
D. GSEA for GO_ ETC Complex Assembly as for Panel (A)
E. GSEA for GO_ Cellular Respiration as for Panel (A)
F. GSEA for GO_ Electron Transport Chain as for Panel (A)
G. GSEA for GO_ Energy Derived by Oxidation as for Panel (A)
H. GSEA for GO_ Energy Generation as for Panel (A)
I. GSEA for GO_ Organic Acid Catabolic Process as for Panel (A)
J. GSEA for GO_ Digestive System Process as for Panel (A)
K. RNA expression of *Prkaa1* was detected by RNA scope using RNAscope 2.5 HD-Brown kit. Images were taken under high magnification (40X) on an Olympus BX43 light microscope, post-imaging adjustments and stitching were performed with Adobe Photoshop CS6. *Prkaa1* showed sparser labeling overall with slight enrichment in PCs but some labeling also in isthmal/pit cells. Boxed area showed pit, isthmus, neck and bottom zone of stomach glands respectively. Scale bar, 30 μm.
L. RNA scope of *Prkaa2* RNA expression as for Panel (A), *Prkaa2* RNA was expressed in parietal cells and scattered labeling in other cells, in particular isthmal progenitor and pit cells. Boxed area showed pit, isthmus, neck and bottom zone of stomach glands respectively. Scale bar, 30 μm.

Figure S2. Metformin increases parietal cell census, Related to Figure 2

A. H&E of stomach corpus glands after 14 days ±metformin (MET) at homeostasis. Note the epithelium was thickened in metformin treated mice with increased parietal cells. Scale bar, 30 μm.
B. Mice were treated as follows: pre-treatment stage: 7 days gavage of 300mg/kg or 3mg/ml in drinking water metformin(MET)/vehicle(VEH); Injury stage: 3 days gavage of 300mg/kg or 3mg/ml in drinking water metformin/vehicle alongside 250mg/kg high-dose tamoxifen (TAM) *i.p.* injection.
C. Mice were treated as follows: pre-treatment stage: 7 days gavage of 300mg/kg or 3mg/ml in drinking water metformin/vehicle; Injury stage: 3 days gavage of 300mg/kg or 3mg/ml in drinking water metformin/vehicle alongside 250mg/kg tamoxifen *i.p.* injection; Recovery stage: 4 days gavage of 300mg/kg or 3mg/ml in drinking water metformin/vehicle.
D. Mice were treated as follows: pre-treatment stage: 7 days gavage of 300mg/kg or 3mg/ml in drinking water metformin/vehicle; Injury stage: 3 days gavage of 300mg/kg or 3mg/ml in drinking water metformin/vehicle alongside 250mg/kg tamoxifen *i.p.* injection; Recovery stage: 11 days gavage of 300mg/kg or 3mg/ml in drinking water metformin/vehicle.
E. H&E of stomach corpus glands after high-dose tamoxifen 14 days ±metformin treatment showing that metformin increased parietal cell (arrowheads) number (details of mouse treatment is shown in Figure S4B). Scale bar, 30 μm.
F. H&E of wildtype mice stomachs after 3 days high dose tamoxifen ± 3 days metformin treatment (details of mouse treatment is shown in Figure S4A). Note both conditions exhibited similar damage and metaplastic change with equivalent chief cell loss (manifested as gland dropout) and parietal cell loss. Scale bar, 30 μm.
G. Quantification of surviving parietal cells after tamoxifen injury as in Panel (A). Note, metformin did not affect parietal cell ablation from tamoxifen treatment. Statistical information: datapoints represent the mean value of parietal cells per gastric unit from ≥70 gastric units counted in an individual mouse. Significance calculated using two-tailed Student's *t*-test.
H. Immunohistochemistry images of gastric intrinsic factor (GIF) staining of wildtype mice stomachs after 3 days tamoxifen ± 3 days metformin treatment. Chief cells underwent paligenosis equivalently in both genotypes with scant GIF left in metaplastic cells at the base. Some GIF label is of extruded cell debris. Scale bar, 30 μm.
I. Immunohistochemistry of the metaplastic marker, SOX9, which is induced in paligenotic chief cells after 3 days tamoxifen ± 3 days metformin treatment. Note SOX9 induction was

not affected by metformin treatment. Boxed areas magnified in insets. Scale bar, 30 μm; inset, 15 μm.

J. Table displaying turnover time and percentage of proliferation needed to maintain cell population at homeostasis for 14 days. Turnover time based on altered calculations from Karam and Leblond, 1993b and observed cell census at homeostasis ± 14 days of metformin.

K. Representative immunofluorescence of proliferation marker EdU after 3 days tamoxifen ± 3 days metformin treatment and 36 hour EdU pulse. Note, the pit region of the gland in metformin-treated mouse retained EdU label (green) whereas few cells in pit region of vehicle-treated mouse retained label as highlighted in boxed images. Pit cells were stained with Muc5AC (not shown here). Scale bar, 20 μm

Figure S3. Metformin decreases proliferation and increases relative parietal cell lineage *ex vivo* in gastric organoids, Related to Figure 3

A. H&E of growing 1st generation gastroids derived from *Atp4b-cre;ROSA mT/mG* mice. Gastroids were treated with vehicle or metformin for 7 days. Parietal cells are typically slowly lost in organoid culture. Single surviving parietal cells are outlined in boxed area; they were characterized by large size, large nuclei and abundant, eosinophilic (pink) cytoplasm with cleared apical membrane folds. Note, from the representative organoids depicted, metformin-treated gastroids had increased parietal cell survival but decreased overall growth compared to control gastroids. Scale bar, 500 μm; inset, 200 μm.
B. H&E of 2nd generation gastroids derived from *Atp4b-cre;ROSA mT/mG* mice. 2nd generation gastroids were passaged from untreated 1st generation *Atp4b-cre;ROSA mT/mG* gastroids and treated with metformin or vehicle for 7 days. Note, both parietal lineage and non-parietal lineage cells were able to form gastroids. Single parietal lineage and non-parietal lineage cells are isolated by boxes. Scale bar, 500 μm; inset, 200 μm.
C. Dose curve of metformin on gastroid size normalized to control treatment of no metformin. Concentration is expressed logarithmically. Compound C concentration was 5mM. Statistical information: datapoints represent the mean diameter of gastroids normalized to an untreated control for each concentration. Significance calculated using a one-tailed, paired Student's *t*-test of the area under the curve comparing inhibitor-treated vs. metformin-only-dosed curves for organoids derived from a single mouse; both curves with left boundary dictated by vehicle-treatment. The black line represents the mean for each concentration.
D. Experiment in (C) repeated to confirm effect of Compound C on highest dose of metformin and to determine effects of Compound C (5 mM) alone on gastroid size. Data are all normalized to untreated control. Statistical information: datapoints represent the mean diameter of gastroids from a single mouse normalized to mean diameter of untreated organoids for the same mouse. Significance calculated using one way ANOVA with Dunnett's multiple comparison post hoc correction.
E. Immunofluorescence for proliferating cells (BrdU, white) and parietal cells (VEGFB, green) in vehicle or metformin treated 1st generation *Atp4b-cre;ROSA mT/mG* gastroids. Red arrows: $VEGFB^+$ parietal cells in 1st generation gastroids. Nuclei are stained blue with DAPI. Note metformin decreased proliferative cells and increased parietal cell census. Scale bar, 50 μm; inset, 20 μm.
F. Immunofluorescence as for panel (A) in 2nd generation, parietal-cell-lineage (green gastroids from Figure 3D) and non-parietal-cell lineages (red in Figure 3D). Metformin decreased

proliferating cells in both types of gastroids. Parietal cells in metformin treatment tended to be larger than in control. Nuclei are stained blue with DAPI. Scale bar, 50 μm; inset, 20 μm.

Figure S4. *Ppargc1*$^{-/-}$ stomachs display no change in lineage allocation, but PC-specific loss of AMPKα decreases PC census, Related to Figure 4 and Figure 5

A. H&E of untreated *Ppargc1*$^{-/-}$ *and Ppargc1*$^{+/+}$ control mice stomach glands at homeostasis. Parietal cells frequently had stunted or abnormal ezrin networks in *Ppargc1*$^{-/-}$ mice. Scale bar, 30 μm.
B. Immunohistochemistry showing DBA staining of *Ppargc1*$^{-/-}$ *and Ppargc1*$^{+/+}$ control mice stomach glands as for panel (A). Scale bar, 30 μm.
C. Immunohistochemistry showing Mucin 5ac staining of *Ppargc1*$^{-/-}$ *and Ppargc1*$^{+/+}$ control mice stomach glands as for panel (A). Scale bar, 30 μm.
D. Immunohistochemistry showing GSII staining of *Ppargc1*$^{-/-}$ *and Ppargc1*$^{+/+}$ control mice stomach glands as for panel (A). Scale bar, 30 μm.
E. Immunohistochemistry showing GIF staining of *Ppargc1*$^{-/-}$ *and Ppargc1*$^{+/+}$ control mice stomach glands as for panel (A). Scale bar, 30 μm.
F. H&E of *Atp4b-cre;Prkaa1*$^{\Delta/\Delta}$*;Prkaa2*$^{\Delta/\Delta}$ and *Atp4b-cre* control stomach corpus in homeostasis. *Atp4b-cre;Prkaa1*$^{\Delta/\Delta}$*;Prkaa2*$^{\Delta/\Delta}$ mice had decreased parietal cell number. Scale bar, 30 μm.
G. Immunohistochemistry for parietal-cell-enriched protein Ezrin with mice as for panel (A). Note *Atp4b-cre;Prkaa1*$^{\Delta/\Delta}$*;Prkaa2*$^{\Delta/\Delta}$ mice had decreased parietal cell number. Scale bar, 30 μm.
H. Quantification of the distance from nucleus to margin of *Atp4b-cre;Prkaa1*$^{\Delta/\Delta}$*;Prkaa2*$^{\Delta/\Delta}$ and *Atp4b-cre* control mice in homeostasis. Note parietal cells in *Atp4b-cre;Prkaa1*$^{\Delta/\Delta}$*;Prkaa2*$^{\Delta/\Delta}$ stomach exhibited a more eccentric nuclear position which indicated a less developed status, as parietal cell nuclei become centralized as they mature. Statistical information: datapoints represent distance for a single parietal cell, all collected from ≥200 parietal cells across three mice. Significance calculated using one-tailed Student's *t*-test.

Figure S5: Metformin enriches genesets associated with energetics in wildtype mice, but enriches genesets for development and stem cell differentiation in AMPK-deficient mice, Related to Figure 6

A. GO Genesets with highest Normalized Enrichment Score (NES) in Meformin (METD14) treated wildtype mice compared to the vehicle (VEHD14) treated control was shown in Figure 6A: GO_ Oxidative Phosphorylation
B. GSEA for GO_ Mitochondrial Respiratory Chain Complex Assembly as for Figure 6A
C. GSEA for GO_ Electron Transport Chain as for Figure 6A
D. GSEA for GO_ Mitochondrial Respiratory Chain Complex1 Biogenesis as for Figure 6A
E. GSEA for GO_ Mitochondrial Translation as for Figure 6A
F. GO Genesets with highest Normalized Enrichment Score (NES) in Metformin (METD14) treated *Atp4b-cre;Prkaa1*$^{\Delta/\Delta}$*;Prkaa2*$^{\Delta/\Delta}$ mice (AMPK mutant METD14) compared to the vehicle (VEHD14) treated *Atp4b-cre;Prkaa1*$^{\Delta/\Delta}$*;Prkaa2*$^{\Delta/\Delta}$ mice (AMPK mutant VEHD14) was shown in Figure 6B: GO_ Epidermis Development
G. GSEA for GO_ Epithelial Cell Differentiation as for Figure 6B
H. GSEA for GO_ Morphogenesis of an Epithelium as for Figure 6B
I. GSEA for GO_ Tissue Development as for Figure 6B
J. GSEA for GO_ Embryonic Development as for Figure 6B

Figure S6. PC-specific loss of AMPKα and *Ppargc1* decreases PC census and maturity, Related to Figure 5, Figure 6, and Figure 7

A. Representative bright field image of gastroid derived from *Atp4b-cre;Prkaa1$^{\Delta/\Delta}$;Prkaa2$^{\Delta/\Delta}$* and *Atp4b-cre* control mice treated for 7 days ± metformin. Scale bar, 200 μm.
B. Quantification of diameter of 1st generation gastroids as for panel (A). Statistical information: datapoints represent the mean gastroid diameter of ~50 gastroids from an individual mouse. Significance calculated using tw
C. H&E of *Atp4b-cre;Ppargc1 $^{\Delta/\Delta}$* and *Atp4b-cre* control stomach corpus in homeostasis. *Atp4b-cre;Ppargc1 $^{\Delta/\Delta}$* mice had decreased parietal cell number. Scale bar, 30 μm.
D. Immunohistochemistry for parietal-cell-enriched protein Ezrin with mice as for panel (A). Note, *Atp4b-cre;Ppargc1 $^{\Delta/\Delta}$* mice had decreased parietal cell number. Scale bar, 30 μm.
E. Quantification of the distance from nucleus to margin of *Atp4b-cre;Ppargc1 $^{\Delta/\Delta}$* and *Atp4b-cre* control mice in homeostasis. Note parietal cells in *Atp4b-cre;Ppargc1 $^{\Delta/\Delta}$* stomach exhibited a more eccentric nuclear position which indicated a less developed status, as parietal cell nuclei become centralized as they mature. Statistical information: datapoints represent distance for a single parietal cell, all collected from ≥225 parietal cells across three mice. Significance calculated using one-tailed Student's *t*-test.
F. Quantification of gastric juice pH value of *Atp4b-cre;Ppargc1 $^{\Delta/\Delta}$ and Atp4b-cre* control mice. pH value was significantly increased in *Atp4b-cre;Ppargc1 $^{\Delta/\Delta}$* mice. Statistical information: datapoints represent pH value from an individual mouse. Significance was calculated using two-tailed Student's *t*-test.
G. Immunofluorescence for parietal cells (Ezrin, green) and ribosomal protein S6 phosphorylated at the 240/244 residues indicating mTORC1 activation (red) in *Atp4b-cre;Prkaa1$^{\Delta/\Delta}$;Prkaa2$^{\Delta/\Delta}$, Atp4b-cre;Ppargc1$^{\Delta/\Delta}$* or *Atp4b-cre* control mice at homeostasis. Note, as opposed to control PCs, both mutant mice had parietal cells exhibiting cytoplasmic pS6 240/24, indicating mutant PCs aberrantly activated mTORC1. Nuclei are stained blue with DAPI. Scale bar, 30 μm; inset, 15 μm.
H. Transmission electron microscopy of control and mutant mice in homeostasis. Note mitochondria (eg, outlined in yellow) in parietal cells of both mutants showed morphology with pinched, twisted morphology and disordered cristae (*upper row*). Free ribosomes (arrows) accumulated in both mutants (lower row), whereas free ribosomes are rare in wildtype parietal cells; ribosomogenesis is consistent with increased mTORC1. Lysosomes (eg outlined in red) in control parietal cells were globular and adjacent to mitochondria, as we have shown previously in Lo et al., 2018. In mutants,

lysosomes were irregular in size and shape and often not near mitochondria. Scale bar, 1 μm.

Figure S7. Metformin no longer affects parietal cell maturation in mice with PC-specific AMPK deletion but still significantly decreases progenitor cell proliferation, Related to Figure 6

A. H&E of *Atp4b-cre;Prkaa1$^{\Delta/\Delta}$;Prkaa2$^{\Delta/\Delta}$* and *Atp4b-cre* control mice after high dose tamoxifen (TAM) ±7 days metformin. Note mutant mice had decreased parietal cell (eg arrowheads) number and size compared to control animal when treated with vehicle or metformin. Scale bar, 30 μm.
B. Quantification of stomach gastric juice pH value in control and mutant mice as treated in panel (A). Note pH increased in the *Atp4b-cre;Prkaa1$^{\Delta/\Delta}$;Prkaa2$^{\Delta/\Delta}$* mice, consistent with decreased parietal cell function. Metformin caused increased parietal cell function in *Atp4b-cre* control mice as measured by gastric pH but could not decrease pH in mutant, consistent with effects of metformin on parietal cell being governed by AMPK. Statistical information: datapoints represent pH value from an individual mouse. Significance calculated using one-tailed Student's *t*-test as the groups were independently compared.
C. Quantification of nuclear eccentricity *Atp4b-cre;Prkaa1$^{\Delta/\Delta}$;Prkaa2$^{\Delta/\Delta}$* and *Atp4b-cre* control mouse parietal cells treated as in panel (A). Note parietal cells in *Atp4b-cre;Prkaa1$^{\Delta/\Delta}$;Prkaa2$^{\Delta/\Delta}$* mice exhibited a more eccentric nuclear position when treated with vehicle alone compared to vehicle treated wildtype control, consistent with immaturity. Statistical Information: Statistical information: datapoints represent distance for a single parietal cell, all collected from ≥30 parietal cells across three mice. Significance calculated using one-tailed Student's *t*-test as the groups were independently compared.
D. Immunofluorescence of *Atp4b-cre;Ppargc1$^{\Delta/\Delta}$* and *Atp4b-cre* control mice after high dose tamoxifen (TAM) ±7 days metformin. Parietal cells (red, VEGFB); mucous neck cells (green, GSII); nuclei (blue, DAPI). Metformin did not affect abnormal parietal cell morphology or census in mutant animals compared to vehicle treated mutant. Scale bar, 30 μm
E. H&E of *Atp4b-cre;Ppargc1$^{\Delta/\Delta}$* and *Atp4b-cre* control mice after high dose tamoxifen (TAM) ±7 days metformin. Note, *Atp4b-cre;Ppargc1$^{\Delta/\Delta}$* mice had decreased parietal cell number and size compared to control animal when treated with vehicle or metformin. Scale bar, 30 μm.
F. Quantification of parietal cell size (diameter) *Atp4b-cre;Ppargc1$^{\Delta/\Delta}$* and *Atp4b-cre* control mouse parietal cells treated as in panel (A). Note parietal cells in *Atp4b-cre;Ppargc1$^{\Delta/\Delta}$* mice exhibited a smaller size when treated with vehicle alone compared to vehicle treated wildtype control, consistent with immaturity; however Metformin did not increase parietal diameter in *Atp4b-cre;Ppargc1$^{\Delta/\Delta}$* mouse compared to vehicle-treated *Atp4b-cre;Ppargc1$^{\Delta/\Delta}$* mouse. Statistical information: datapoints represent the mean parietal cell size from ≥50

parietal cells counted in an individual mouse. Significance calculated using one-tailed Student's *t*-test as the groups were independently compared.

G. Quantification of stomach gastric juice pH value in *Atp4b-cre;Ppargc1*$^{\Delta/\Delta}$ and *Atp4b-cre* control mice as treated in panel (A). Note pH increased in *Atp4b-cre;Ppargc1*$^{\Delta/\Delta}$ mouse, consistent with decreased parietal cell function. Metformin increased parietal cell function in *Atp4b-cre* control mice as measured by gastric pH but could not decrease pH in *Atp4b-cre;Ppargc1*$^{\Delta/\Delta}$ mouse, consistent with effects of metformin on parietal cell being governed by AMPK. Statistical information: datapoints represent pH value from an individual mouse. Significance calculated using one-tailed Student's *t*-test as the groups were independently compared.

H. Quantification of nuclear eccentricity of *Atp4b-cre;Ppargc1*$^{\Delta/\Delta}$ and *Atp4b-cre* control mouse parietal cells treated as in panel (A). Note parietal cells in *Atp4b-cre;Ppargc1*$^{\Delta/\Delta}$ mice exhibited a more eccentric nuclear position when treated with vehicle alone compared to vehicle treated wildtype control, consistent with immaturity. Statistical information: datapoints represent distance for a single parietal cell, all collected from ≥30 parietal cells across three mice. Significance calculated using one-tailed Student's *t*-test as the groups were independently compared.

Figure S1

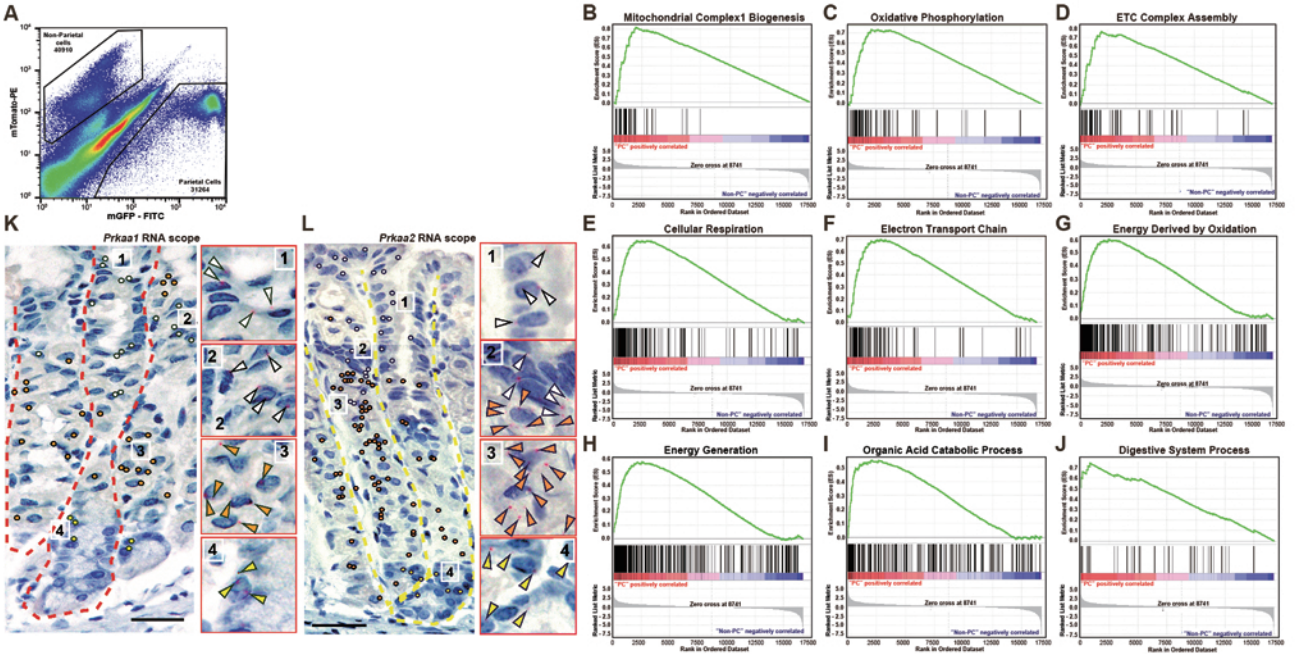
A
Non-Parietal cells 40910
Parietal Cells 31264
mTomato-PE
mGFP - FITC
B
Mitochondrial Complex1 Biogenesis
C
Oxidative Phosphorylation
D
ETC Complex Assembly
E
Cellular Respiration
F
Electron Transport Chain
G
Energy Derived by Oxidation
H
Energy Generation
I
Organic Acid Catabolic Process
J
Digestive System Process
Enrichment Score (ES)
Ranked List Metric
Rank in Ordered Dataset
"PC" positively correlated
"Non-PC" negatively correlated
Zero cross at 8741
K
Prkaa1 RNA scope
L
Prkaa2 RNA scope

Figure S2

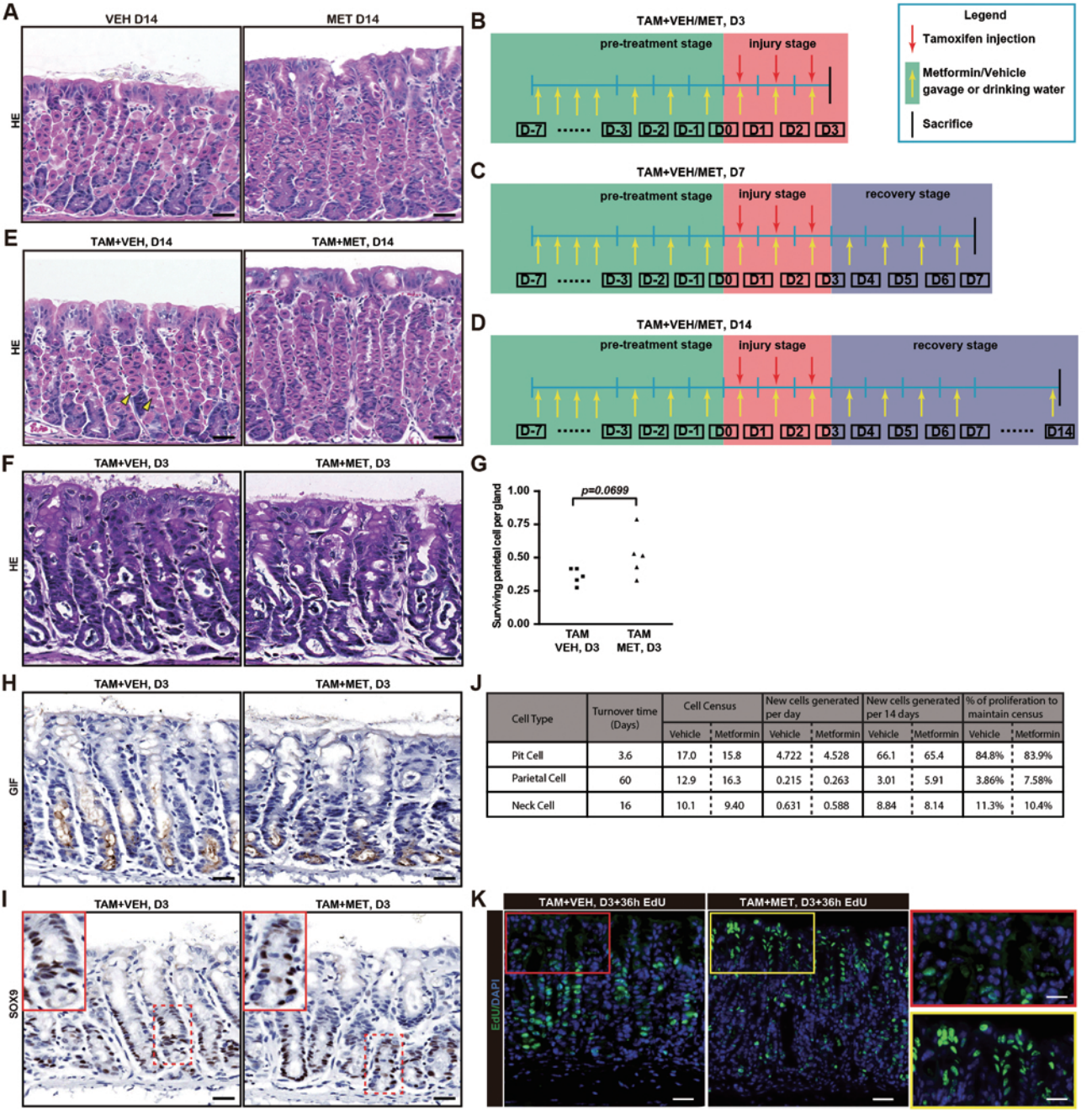

J

Cell Type	Turnover time (Days)	Cell Census		New cells generated per day		New cells generated per 14 days		% of proliferation to maintain census	
		Vehicle	Metformin	Vehicle	Metformin	Vehicle	Metformin	Vehicle	Metformin
Pit Cell	3.6	17.0	15.8	4.722	4.528	66.1	65.4	84.8%	83.9%
Parietal Cell	60	12.9	16.3	0.215	0.263	3.01	5.91	3.86%	7.58%
Neck Cell	16	10.1	9.40	0.631	0.588	8.84	8.14	11.3%	10.4%

Figure S3

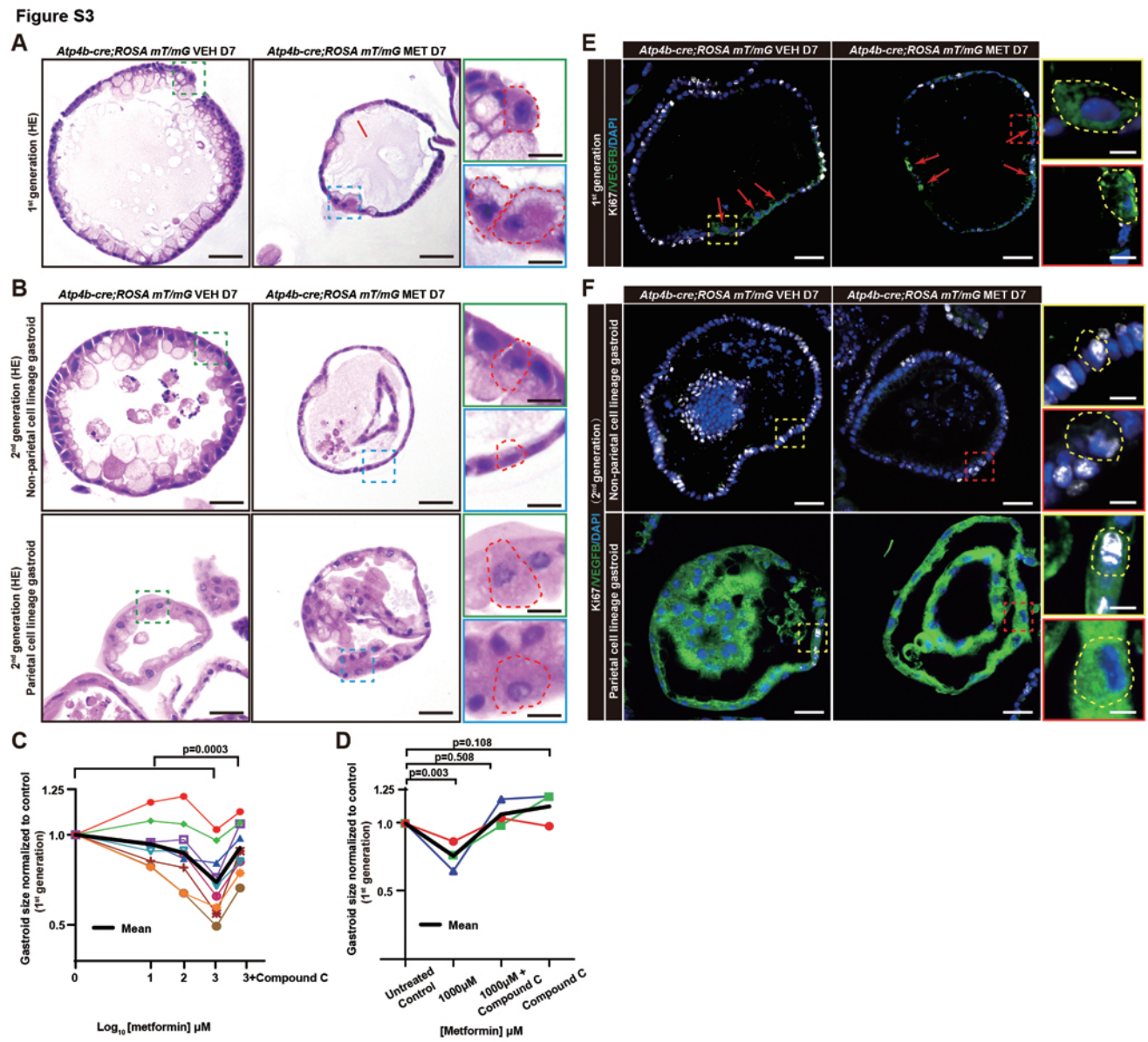
A
Atp4b-cre;ROSA mT/mG VEH D7
Atp4b-cre;ROSA mT/mG MET D7
1st generation (HE)
B
Atp4b-cre;ROSA mT/mG VEH D7
Atp4b-cre;ROSA mT/mG MET D7
2nd generation (HE)
Non-parietal cell lineage gastroid
2nd generation (HE)
Parietal cell lineage gastroid
C
p=0.0003
Gastroid size normalized to control
(1st generation)
1.25
1.0
0.5
Mean
0
1
2
3
3+Compound C
Log10 [metformin] μM
D
p=0.108
p=0.508
p=0.003
Gastroid size normalized to control
(1st generation)
1.25
1.0
0.5
Mean
Untreated Control
1000μM
1000μM + Compound C
Compound C
[Metformin] μM
E
Atp4b-cre;ROSA mT/mG VEH D7
Atp4b-cre;ROSA mT/mG MET D7
1st generation
Ki67/VEGFB/DAPI
F
Atp4b-cre;ROSA mT/mG VEH D7
Atp4b-cre;ROSA mT/mG MET D7
(2nd generation)
Non-parietal cell lineage gastroid
Ki67/VEGFB/DAPI
Parietal cell lineage gastroid

Figure S4

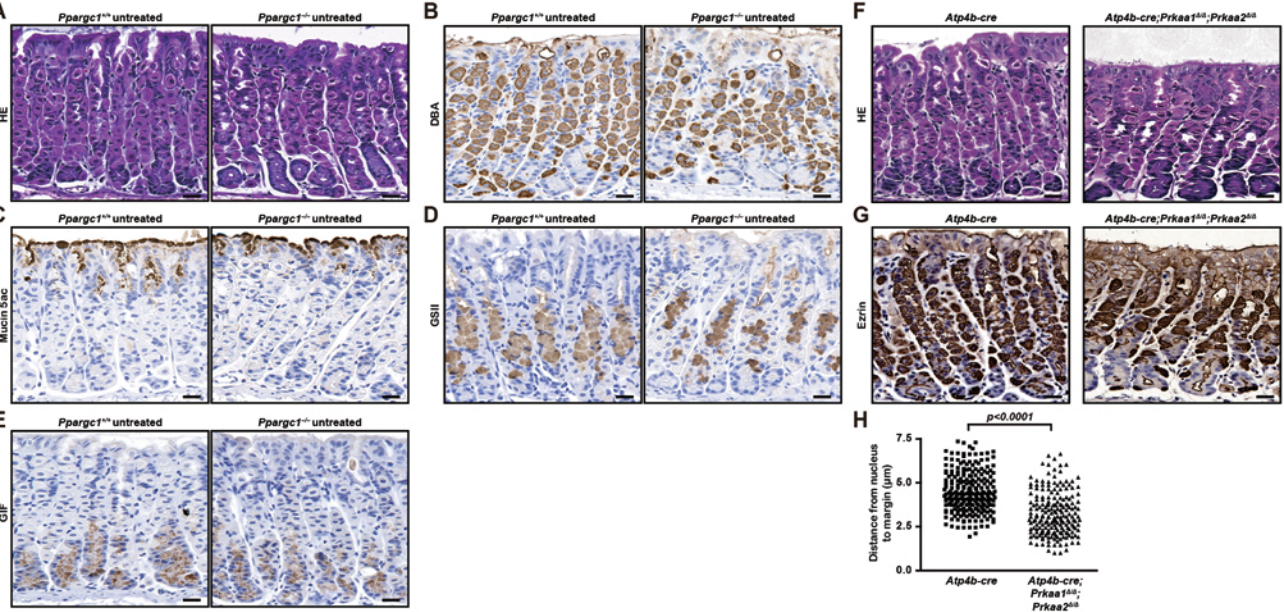
A
Ppargc1a+/+ untreated
Ppargc1a−/− untreated
HE
B
Ppargc1a+/+ untreated
Ppargc1a−/− untreated
DBA
C
Ppargc1a+/+ untreated
Ppargc1a−/− untreated
Mucin 5ac
D
Ppargc1a+/+ untreated
Ppargc1a−/− untreated
GSII
E
Ppargc1a+/+ untreated
Ppargc1a−/− untreated
GIF
F
Atp4b-cre
Atp4b-cre;Prkaa1Δ/Δ;Prkaa2Δ/Δ
HE
G
Atp4b-cre
Atp4b-cre;Prkaa1Δ/Δ;Prkaa2Δ/Δ
Ezrin
H
p<0.0001
Distance from nucleus to margin (μm)
7.5
5.0
2.5
0.0
Atp4b-cre
Atp4b-cre; Prkaa1Δ/Δ; Prkaa2Δ/Δ

Figure S5

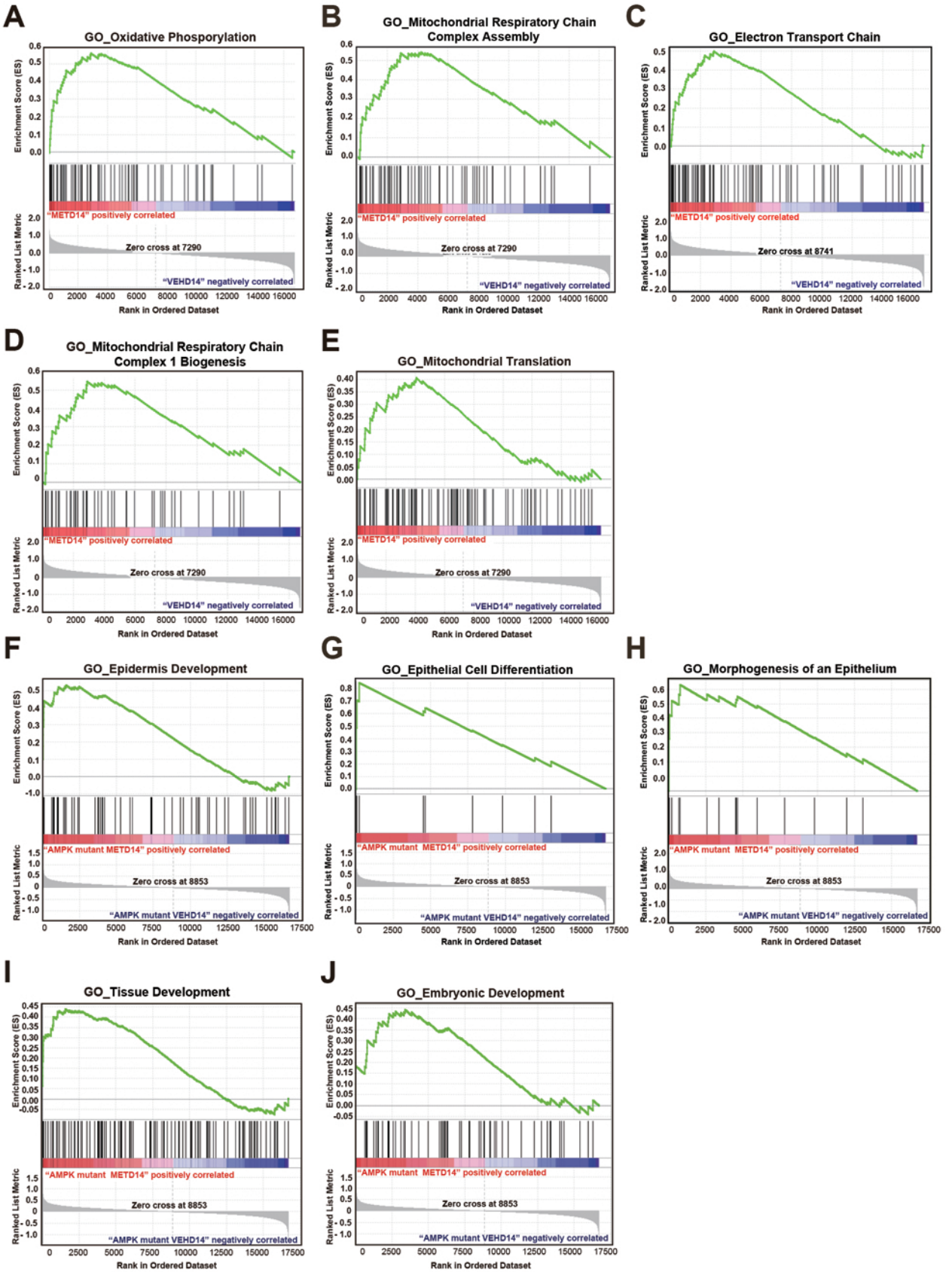
A
GO_Oxidative Phosporylation
B
GO_Mitochondrial Respiratory Chain Complex Assembly
C
GO_Electron Transport Chain
D
GO_Mitochondrial Respiratory Chain Complex 1 Biogenesis
E
GO_Mitochondrial Translation
F
GO_Epidermis Development
G
GO_Epithelial Cell Differentiation
H
GO_Morphogenesis of an Epithelium
I
GO_Tissue Development
J
GO_Embryonic Development
Enrichment Score (ES)
Ranked List Metric
Rank in Ordered Dataset
"METD14" positively correlated
"VEHD14" negatively correlated
"AMPK mutant METD14" positively correlated
"AMPK mutant VEHD14" negatively correlated
Zero cross at 7290
Zero cross at 8741
Zero cross at 8853

Figure S6

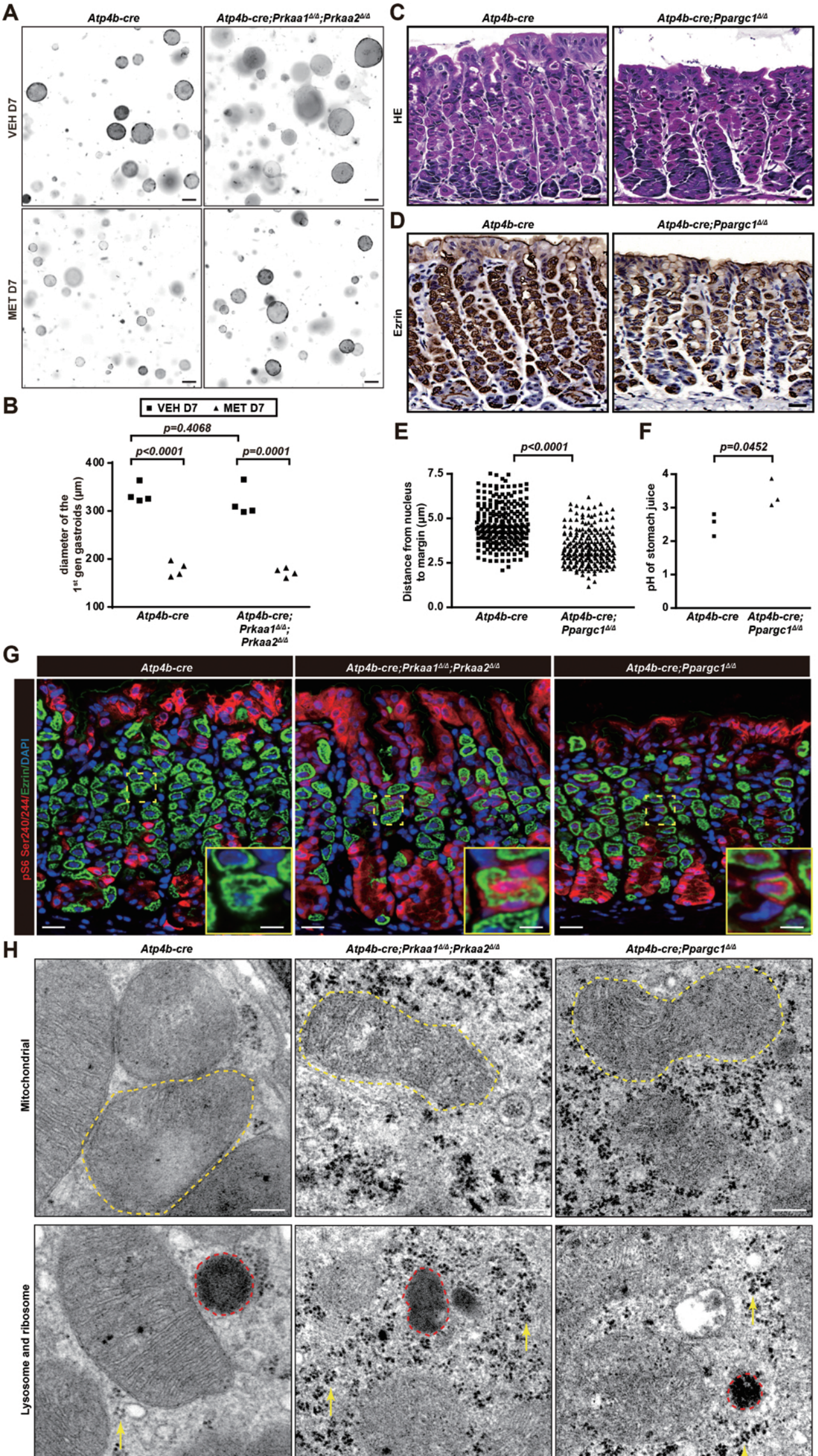
A
Atp4b-cre
Atp4b-cre;Prkaa1Δ/Δ;Prkaa2Δ/Δ
VEH D7
MET D7
C
Atp4b-cre
Atp4b-cre;Ppargc1Δ/Δ
HE
D
Atp4b-cre
Atp4b-cre;Ppargc1Δ/Δ
Ezrin
B
VEH D7
MET D7
p=0.4068
p<0.0001
p=0.0001
diameter of the 1st gen gastroids (μm)
400
300
200
100
Atp4b-cre
Atp4b-cre; Prkaa1Δ/Δ; Prkaa2Δ/Δ
E
p<0.0001
Distance from nucleus to margin (μm)
7.5
5.0
2.5
0.0
Atp4b-cre
Atp4b-cre; Ppargc1Δ/Δ
F
p=0.0452
pH of stomach juice
4
3
2
1
0
Atp4b-cre
Atp4b-cre; Ppargc1Δ/Δ
G
Atp4b-cre
Atp4b-cre;Prkaa1Δ/Δ;Prkaa2Δ/Δ
Atp4b-cre;Ppargc1Δ/Δ
pS6 Ser240/244/Ezrin/DAPI
H
Atp4b-cre
Atp4b-cre;Prkaa1Δ/Δ;Prkaa2Δ/Δ
Atp4b-cre;Ppargc1Δ/Δ
Mitochondrial
Lysosome and ribosome

Figure S7

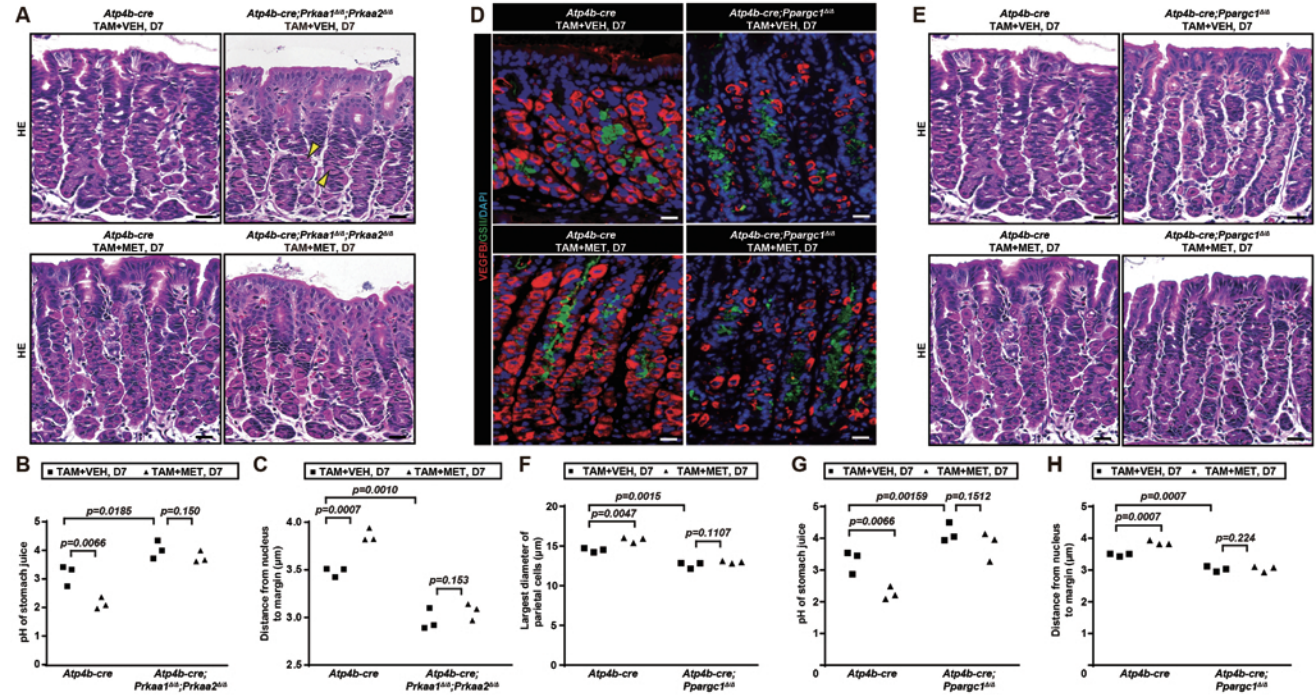
A
Atp4b-cre
TAM+VEH, D7
Atp4b-cre;Prkaa1Δ/Δ;Prkaa2Δ/Δ
TAM+VEH, D7
HE
Atp4b-cre
TAM+MET, D7
Atp4b-cre;Prkaa1Δ/Δ;Prkaa2Δ/Δ
TAM+MET, D7
HE
D
Atp4b-cre
TAM+VEH, D7
Atp4b-cre;Ppargc1Δ/Δ
TAM+VEH, D7
VEGFB/GSII/DAPI
Atp4b-cre
TAM+MET, D7
Atp4b-cre;Ppargc1Δ/Δ
TAM+MET, D7
E
Atp4b-cre
TAM+VEH, D7
Atp4b-cre;Ppargc1Δ/Δ
TAM+VEH, D7
HE
Atp4b-cre
TAM+MET, D7
Atp4b-cre;Ppargc1Δ/Δ
TAM+MET, D7
HE
B
TAM+VEH, D7
TAM+MET, D7
pH of stomach juice
p=0.0185
p=0.150
p=0.0066
Atp4b-cre
Atp4b-cre;Prkaa1Δ/Δ;Prkaa2Δ/Δ
C
TAM+VEH, D7
TAM+MET, D7
Distance from nucleus to margin (μm)
p=0.0010
p=0.0007
p=0.153
Atp4b-cre
Atp4b-cre;Prkaa1Δ/Δ;Prkaa2Δ/Δ
F
TAM+VEH, D7
TAM+MET, D7
Largest diameter of parietal cells (μm)
p=0.0015
p=0.0047
p=0.1107
Atp4b-cre
Atp4b-cre;Ppargc1Δ/Δ
G
TAM+VEH, D7
TAM+MET, D7
pH of stomach juice
p=0.00159
p=0.1512
p=0.0066
Atp4b-cre
Atp4b-cre;Ppargc1Δ/Δ
H
TAM+VEH, D7
TAM+MET, D7
Distance from nucleus to margin (μm)
p=0.0007
p=0.0007
p=0.224
Atp4b-cre
Atp4b-cre;Ppargc1Δ/Δ

Supplementary Table Legends

Table S1

AMPK related genes enriched in parietal cells

Table S2

Metformin D14 all lineage quantification

Table S3

Genotyping primers

Table S4

Antibodies Source and application

Table S5

qPCR primers

Table S6

Statistical Breakdown

Table S7

Markers of various stomach cell type

Table S1. Gene expression of AMPK related genes enriched in parietal cell population, Related to Figure S1

Gene Name	Gene ID	Fold change compared to non-Parietal cells
Ppargc1α	ENSMUSG00000029167	22.905
Ascl1	ENSMUSG00000018796	9.309
Acacb	ENSMUSG00000042010	4.080
Prkaa2	ENSMUSG00000028518	3.526
Stradb	ENSMUSG00000026027	2.585
Prkab2	ENSMUSG00000038205	2.152
Strada	ENSMUSG00000069631	2.146
Prkag1	ENSMUSG00000067713	2.006
Cpt1a	ENSMUSG00000024900	1.853
Slc25a20	ENSMUSG00000032602	1.541
Prkag2	ENSMUSG00000028944	1.456
Cab39	ENSMUSG00000036707	1.365
Stk11	ENSMUSG00000003068	1.345
Prkaa1	ENSMUSG00000050697	1.284
Ppm1a	ENSMUSG00000021096	1.252
Rptor	ENSMUSG00000025583	1.194
Cpt2	ENSMUSG00000028607	1.155
Prkab1	ENSMUSG00000029513	0.723

Table S2. Changes in cell lineage allocation in metformin treated mice, Related to Figure 1E

Cell Type	**D14 Vehicle-treated (Cells per unit ±SEM)**	**D14 Metformin-treated (Cells per unit ±SEM)**
Pit cell	17.02 ±0.28	16.29 ±0.65
Parietal Cell	12.93 ±1.40	15.79 ±1.62
Mucous Neck Cell	10.07 ±0.13	9.35 ±0.25
Chief Cell	8.63 ±0.59	9.24 ±0.17
Total Cell number	48.59 ±1.67	50.68 ±2.10

Table S3. Genotyping primers, Related to STAR Methods

mice name	primer	Sequence
Atp4b-cre	Common Forward	AGG GAT CGC CAG GCG TTT TC
	Common Reverse	GTT TTC TTT TCG GAT CCG CC
Rosa mT/mG	Common Forward	AAG GGA GCT GCA GTG GAG TA
	WT Reverse	CCG AAA ATC TGT GGG AAG TC
	Mutant Reverse	CGG GCC ATT TAC CGT AAG TTA T
Prkaa1$^{flox/flox}$	Common Forward	CCC ACC ATC ACT CCA TCT CT
	Common Reverse	AGC CTG CTT GGC ACA CTT AT
Prkaa2$^{flox/flox}$	Common Forward	GCA GGC GAA TTT CTG AGT TC
	Common Reverse	TCC CCT TGA ACA AGC ATA CC
Ppargc1$^{flox/flox}$	Common Forward	TCC AGT AGG CAG AGA TTT ATG AC
	Common Reverse	TGT CTG GTT TGA CAA TCT GCT AGG TC

Table S4. Antibodies Source and application, Related to STAR Methods

Antibody	Source	application	dilution
Brdu	DSHB (G3G4)	IF, IHC	1:100
VEGFb	Santa Cruz (sc-1876)	IF	1:100
GIF	gift of Dr. David Alpers, WUSTL	IF, IHC	1:10000
LKB1	Santa Cruz (sc-32245)	IHC	1:200
AMPKα	Cell Signaling (#2532)	WB	1:1000
AMPKα2	Sigma-Aldrich (HPA044540)	IHC	1:200
PGC1α	Abcam(ab54481)	WB, IHC	1:2000 (WB); 1:400 (IF)
Sox9	Millipore (ABE 571)	IHC	1:1500
GFP	Santa Cruz (sc-9996)	IF	1:100
pS6 (240/244)	Cell Signaling (#2215)	IF	1:200
Tubulin	Abcam (ab21057)	WB	1:1000
Ezrin	Santa Cruz (sc-58758)	IF, IHC	1:100
cytochromeC	Abcam (ab13575)	IF	1:200
GSII-Alexa Fluor 647	Invitrogen (L32451)	IF	1:500

Table S5. qPCR primers, Related to STAR Methods

Gene	Primer	Sequence
Prkaa1	Forward	GTCAAAGCCGACCCAATGATA
	Reverse	CGTACACGAAAATAATAGGGGTT
Prkaa2	Forward	CAGGCCATAAAGTGGCAGTTA
	Reverse	AAAAGTCTGTCGGAGTGCTGA
Ppargc1α	Forward	TATGGAGTGACATAGAGTGTGCT
	Reverse	CCACTTCAATCCACCCAGAAAG
Ezrin	Forward	CAATCAACGTCCGGGTGAC
	Reverse	GCCAATCGTCTTTACCACCTGA
Atp4b	Forward	CAGGAGAAGAAGTCATGCAGC
	Reverse	GAAACCTGCGTAGTACAGGCT
VefgB	Forward	GCCAGACAGGGTTGCCATAC
	Reverse	GGAGTGGGATGGATGATGTCAG
TBP	Forward	CAAACCCAGAATTGTTCTCCTT
	Reverse	ATGTGGTCTTCCTGAATCCCT

Table S6. Statistical analysis breakdown of data, Related to STAR Methods

Main	Figure	Description	Statistical test	Tails
	1E	All lineage quant	Unpaired student 's *t*-test	all 2 tailed +SEM
	1G	WT BrdU METD14	Unpaired student 's *t*-test	2-tailed
	2B	HDT+Met qPCR ampka1,2 pgc1a	Unpaired student 's *t*-test	1-tailed+SEM
	2C	HDT+Met qPCR Ezrin, Atp4b, VegfB	Unpaired student 's *t*-test	1-tailed+SEM
	2E	PC number HDT+METD14	Unpaired student 's *t*-test	1-tailed
	2G	WT HDT+MetD14 BrdU	Unpaired student 's *t*-test	1-tailed
	3B	1ST Gen Gastroid diameter	Unpaired student 's *t*-test	1-tailed
	3C	1st gen Green/red ratio	Unpaired student 's *t*-test	1-tailed
	3E	2nd gen gastroid size	Unpaired student 's *t*-test	1-tailed
	4B	KLF4+/Ezrin+ Cell Day14	Unpaired student 's *t*-test	1-tailed
	4D	KLF4+ HDT+METD7	Unpaired student 's *t*-test	1-tailed
	4F	All lineage quant in global PGC1aKO	Unpaired student 's *t*-test	2-tailed+SEM
	4H	Global PGC1a-/- BrdU Untreated	Unpaired student 's *t*-test	2-tailed
	5B	Ampk KO pH	Unpaired student 's *t*-test	2-tailed
	5D	Ampk KO PC number	Unpaired student 's *t*-test	2-tailed
	5F	Ampk KO BrdU	Unpaired student 's *t*-test	2-tailed
	6F	Ampk KO+HDT/METD7 PC number	Unpaired student 's *t*-test	1-tailed
	6G	Ampk KO+HDT/METD7 BrdU	Unpaired student 's *t*-test	1-tailed
	7C	WT DKO PGC1KO Diameter	One-way ANOVA	ANOVA, Dunnett's Multiple comparison post hoc
	7F	WT DKO PGC1KO mitochondria	One-way ANOVA	ANOVA, Dunnett's Multiple comparison post hoc
Supplementary	SF2G	Surviving PC in TAM+/- MetD3	Unpaired student 's *t*-test	2-tailed
	SF3C	Dose Curve	Paired student 's *t*-test on Area Under Curve	1-tailed
	SF3D	Compound C Dose	One-way ANOVA	ANOVA; Dunnett's multiple comparison post hoc
	SF4H	Nucleus margin Ampk KO	Unpaired student 's *t*-test	1-Tailed
	SF6B	Ampk KO Gastroid+METD7	Unpaired student 's *t*-test	2-tailed
	SF6E	Nucleus margin PGC	Unpaired student 's *t*-test	1-tailed
	SF6F	PGC1 KO pH	Unpaired student 's *t*-test	2-tailed
	SF7B	Ampk KO+HDT/METD7 pH	Unpaired student 's *t*-test	1-tailed
	SF7C	Ampk KO+HDT/METD7 Nucleus	Unpaired student 's *t*-test	1-tailed
	SF7F	PGC1K+HDT/METD3 Diameter	Unpaired student 's *t*-test	1-tailed
	SF7G	PGC1K+HDT/METD3 pH	Unpaired student 's *t*-test	1-tailed
	SF7H	PGC1K+HDT/METD3 Nucleus	Unpaired student 's *t*-test	1-tailed

Table S7. Protein markers of various stomach cell type, Related to STAR Methods

Cell type	Marker
Parietal cells	Vegfb
	DBA
	Ezrin
Chief cells	GIF
Pit cells	Mucin 5ac
Neck cells	GSII